STUDY OF THE CORRELATION BETWEEN SOLAR MAGNETIC RECONNECTION FLUX WITH SOLAR FLARE TYPES AND DURATION

BALAMURALIKRISHNA A/L KANNIAH

UNIVERSITI SAINS MALAYSIA

2022

STUDY OF THE CORRELATION BETWEEN SOLAR MAGNETIC RECONNECTION FLUX WITH SOLAR FLARE TYPES AND DURATION

by

BALAMURALIKRISHNA A/L KANNIAH

Thesis submitted in fulfilment of the requirements
for the degree of
Doctor of Philosophy

September 2022

ACKNOWLEDGEMENT

I would like to express my heartfelt thanks to my supervisor, Associate Professor Dr. Abdul Halim Bin Abdul Aziz, for his encouragement and assist me in acquiring an understanding of the subject. Prof. Halim has guided and developed me throughout the past 15 years, from the start of my Masters' degree to the completion of my Ph.D. Likewise, this dissertation would not have been possible without the supervision of Dr. John Soo Yue Han, who led me through each step of the research progress, regularly reviewed my assignment, and enabled me to complete it on time. Dr. John's enthusiasm, patience, dedication, and knowledge are exceptional. I feel honored to be his first Ph.D. student. I am also grateful to my co-supervisor Dr. Norhaslinda Binti Mohamed Tahrin, for her valuable suggestions and guidance. Her distinctly recommendation has made this thesis to be more value-added. I would be amiss if I did not mention my school of physics administrators, Ms. Norazlina Abd Malik and Ms. Dianna Shanti, who were always ready to support and facilitate all my postgraduate administrative chores.

I am eternally grateful for my parents' unconditional love and support. My thesis is dedicated to my loving mother V.Rajammal and beloved late father, Mr. P.Kanniah PJM, PJK, PKT. My deepest thanks to my siblings, Mr. K.Muniesvaran and Mr. K.Sivakumar, who keep me grounded, remind me of what is essential in life, and always support my adventures. Similarly, my kids, S.Mishath, B.Saysshatry, and B.Sidthiq, deserve special recognition for their inspiration in my study. Finally, I owe my deepest gratitude to Thienmoli, who is my love. I am forever thankful for her unconditional love and support throughout my academic years. Last but not least, my thanks to God for all the magic happening around my existence.

TABLE OF CONTENTS

LIST OF TABLES

Page

LIST OF FIGURES

Page

LIST OF APPENDICES

LIST OF ABBREVIATIONS

AR	Active Region
AIA	Atmospheric Imaging Assembly
CME	Coronal Mass Ejection
EM	Emission Measures
EUV	Extreme Ultraviolet
FITS	Flexible Image Transport System
FWHM	Full Width Half Maximum
GOES	Geostationary Operational Environmental Satellites
HMI	Helioseismic and Magnetic Imager
HXR	Hard X-ray Radiation
JSOC	Joint Science Operations Center
NASA	National Aeronautics and Space Administration
NOAA	National Oceanic and Atmospheric Administration
OSO 7	Orbiting Solar Observatory 7
SDO	Solar Dynamics Observatory
SXR	Soft X-ray Radiaotion
WCS	World Coordinate System
XRS	X-ray Sensor
SAO-Image DS9	Smithsonian Astrophysical Observatory

LIST OF SYMBOLS

r	Linear Correlation Coefficient
Å	Angstrom
C	Celsius
K	Kelvin
Hα	Hidrogen alpha
C IV	Carbon IV
Ca II	Calsium II
ω	Angular velocity
u	Velocity
G	Gauss unit
T	Tesla unit
Mx	Maxwell unit

KAJIAN HUBUNGAN ANTARA PENYAMBUNGAN SEMULA FLUKS MEDAN MAGNET SURIA DENGAN JENIS DAN TEMPOH SUAR SURIA

ABSTRAK

Suar suria jenis meletus dan tertutup adalah radiasi elecktromagnet hasil pembebasan tenaga magnet di ruang atmosfera suria. Untuk memahami keciriannya, pekali korelasi linear untuk jumlah fluks penyambungan semula magnet dan tempoh suar berbanding dengan kelas suar mengikut jenis suarnya dicari. Tempoh suar suria diperolehi daripada cerapan satelit 'Geostationary Operational Environmental Satellites' (GOES). GOES mengesan keamatan radiasi suar suria dan mengklasifikasikannnya sebagai A, B, C, M atau X mengikut catitan fluks tertinggi.Sebanyak 33 kejadian suar suria telah dikaji dari kelas M5 hingga X5 dalam lingkungan kedudukan 45° dari garis tengah permukaan suria yang bertarikh antara Februari 2011 hingga September 2017. Suar dikesan menggunakan alat penapisan AIA 1600 Å dengan nilai ambang kiraan 1300. Fluks magnet pula dikesan melalui alat penapisan HMI 6173 Å. Data-data berkenaan diperolehi dari 'Joint Science Operations Center' (JSOC). Kedua-dua imejnya disusunatur dan ditindih bersama untuk mengenal pasti piksel-piksel terang yang baharu (AIA) dan mengira jumlah medan magnet (HMI) yang dirangkuminya.Korelasi linear antara kelas suar berbanding tempoh suar (FWHM) adalah lemah (0.19) sebelum ia diasingkan mengikut jenis suar. Walaubagaimanapun, setelah diasingkan mengikut jenis suar didapati bahawa suar tertutup mempunyai pekali korelasi linear yang lebih tinggi (0.58) daripada suar letusan (0.08) yang tiada sifat korelasi. Tempoh suar kelas M tertutup (0:13:09) adalah kurang daripada separuh tempoh suar letusan (0:28:08).

CME dalam suar letusan berkemungkinan melambatkan penyebaran tenaga disebabkan aktiviti pengstrukturan semula secara besar-besaran oleh fluks magnet di korona. Korelasi linear (0.67) yang berkesan dikenalpasti antara kelas suar dan jumlah fluks sambungan semula magnet secara umum. Namun, suar tertutup mempunyai korelasi linear yang lebih tinggi (0.89) berbanding suar letusan (0.60). Kajian mengikut jenis kelas suar mendedahkan korelasinya hampir berkadar langsung (0.93) dalam suar tertutup kelas-X berbanding dengan suar letusan yang sama kelasnya (0.61). Dipercayai sebahagian daripada tenaga hasil penyambungan semula magnet terbebas sebagai CME semasa suar letusan, manakala suar tertutup menyerap sepenuhnya hasil tenaga tersebut kedalam aktiviti suar. Maka, kelas-X lebih menonjolkan sifat kesan perambatan tenaganya. Suatu kaedah pendekatan dikenalkan untuk menentukan jumlah fluks penyambungan semula magnet. Ia adalah hasil daripada ciri magnetik piksel HMI yang berubah sebanyak 10% antara cerapan. Keputusan kaedah pendekatan rapat berbeza sebanyak 33% berbanding kaedah pengaturcaraan. Namun, dengan menggunakan nilai luas piksel yang diperolehi melalui kaedah pengaturcaraan telah mengurangkan jurangnya kepada 12%. Kaedah pendekatan rapat terbukti berkesan namun ia memerlukan kerja menambahbaikan. Kajian ini dipercayai akan bermanfaat kepada bakal penyelidik dalam mempertimbangkan ciri-ciri jenis suar apabila meneliti parameter-parameter suar suria.

STUDY OF THE CORRELATION BETWEEN SOLAR MAGNETIC RECONNECTION FLUX WITH SOLAR FLARE TYPES AND DURATION

ABSTRACT

Solar flares are eruptive or confined electromagnetic radiation associated with a magnetic energy release in the solar atmosphere. To understand the characteristic, the linear correlation coefficient for total magnetic reconnection flux and flare duration versus flare class by flare type were find. The flare duration was derived from Geostationary Operational Environmental Satellites (GOES). The GOES X-ray sensors detect solar flare intensity and classify them as A, B, C, M, or X according to their peak fluxes. A total of 33 flare events of M5 to X5 flare classes within 45° of Sun's disk center were examined, dated between February 2011 to September 2017. The flare is spotted using the AIA 1600 Å filtergram with a threshold of 1300 count. The magnetic flux was determined via the HMI 6173 Å filtergram. Their data are accessible through the Joint Science Operations Center (JSOC). Both images were co-registered and superimposed to identify the newly brightened pixels (AIA) then calculated the underlying magnetic field (HMI). The linear correlation between flare class against duration by Full Width Half Maximum (FWHM) is weak (0.19) before the segregation by flare types. However, the further breakdown shows confined flares have a higher linear correlations coefficient (0.58) than eruptive (0.08) no correlation. The confined M class flares duration (0:13:09) are less than half of the eruptive flares (0:28:08). The CME associated with the eruptive flares could be delaying the energy propagation because of a massive restructuring of the corona's magnetic flux. A linear correlation (0.67) was identified between flare class and total magnetic reconnection

flux before dividing by flare types. Confined flares have a higher linear correlation (0.89) than eruptive flares (0.60). Further examination by flare class reveals a nearly direct (0.93) correlation in the X-class confined flares than X-class eruptive flares (0.61). Part of the magnetic reconnection energy escaped as a CME during the eruptive flares compared to confined energy is completely absorbed in the flare activity. Thus, the X-class reflects the energy propagation effectively. The manual-approach method was used to determine total magnetic reconnection flux. It relies on the HMI pixel's magnetic characteristic changing by 10% between cadences. The manual-approach method differed by 33% from software results. Using an appropriate pixel's area parameter reduced the discrepancy to 12%. It is a reliable method that requires enhancements to make the MS excel steps easier. This study can benefit future researchers in considering flare type characteristics when examining solar flare parameters.

CHAPTER 1

INTRODUCTION

1.1. Introduction

The Sun is a magnetic and dynamic star. The solar flare is the sudden electromagnetic radiation associated with magnetic energy release. Magnetic reconnection is the fundamental mechanism through which energy stored in magnetic fields is released explosively on a massive scale. They are often associated with corona mass ejections (CMEs), which are the dominant contributors to adverse space weather on Earth. Eruptive events are usually referred to as flares associated with a CME, while flares that a CME does not accompany are referred to as confined events (Svestka & Cliver, 1992). Their occurrence, duration, and strength are measured by the Geostationary Operational Environmental Satellite (GOES) spacecraft defined as GOES X-ray peak intensity. Solar flare characteristics have been extensively studied using GOES XRS critical parameters.

Thus, the subjects covered in this thesis are not new; instead, numerous pieces of prior scholarly study on magnetic reconnection flux and flare duration exist. As such, the current study takes the form of a new investigation that relied on a previous research topic.

1.2 Problem Statement

Veronig et al. (2002) and Reep and Knizhnik (2019) showed a 0.25 and 0.09 linear correlation between duration and flare class before flare type segregation, respectively. Will this relationship hold for both confined and eruptive types of flares? As far as known, there are no data on the linear correlation coefficient recorded for the duration by flare types. Additionally, both studies' sample sizes for the B and C

classes were almost 91% - 95% of their respective populations. Could this skewed sample size reflect the higher flare class characteristics, particularly the 0.2% - 0.5% X-classes? The soft X-ray flux magnitude range for solar flares of the B and C classes is between 10^{-7} and 10^{-5} Wm^{-2}, which is smaller magnitude than the range for flares of the M and X classes, which is between 10^{-5} and 10^{-4} Wm^{-2}.

In another parameter, Veronig and Polanec (2015) and Tschernitz et al. (2018) showed correlation coefficients of 0.78 and 0.92, respectively, on total magnetic reconnection flux against flare classes before separating by flare type. However, after being segregated by flare type, Tschernitz et al. (2018) showed an equally strong linear correlation in confined (0.90) and eruptive flares (0.94), which included extreme flares (X10 and X17). Extreme flares X10 and X17 (10^{-4} Wm^{-2}) are typically 10 to 17 times or 20 to 34 times larger than X1 or M5 flares, respectively. In their population sample sizes, these extreme events are therefore regarded as outlier samples. Additionally, using a log-log plot correlation will result in greater correlation coefficient values. The sample used by Veronig and Polanec (2015) was homogeneous data, where all the 27 events are eruptive types taken from archives to be compared with a single confined X1.6 flare studied. If extreme flares are excluded, will the results remain unchanged, especially by flare type?

1.3 Research Objective

The focus of the study is to determine the strength of the relationship between flare class against total magnetic reconnection flux and flare duration (FHWM) both before and after segregation by confined and eruptive flare type. In this work, using an equally comparable strength sample size without (few) extreme events in both confined and eruptive flares is a statistically important strategy to establish a great

assessment. Therefore, this effort will uncover previously unexplored portions in the correlation of the duration by flare type and reevaluate the correlation outcome without (few) extreme events in the sample size for total magnetic reconnection flux. The objective of the study is to:

1. Determine the relationship between flare duration and flare class. Find the linear correlation coefficient of the magnitude before and after segregated by flare type to compare and understand confined and eruptive flare characteristics related to the duration parameter. Based on literature review, there is no record of correlation coefficient for the flare duration against flare class by flare type reported.

2. Determine the relationship between total magnetic reconnection flux and flare class. Find the linear correlation coefficient magnitude before and after segregating by flare type to compare and understand the characteristics of confined and eruptive flares in the energy transformation. Based on previous studies, their data remains limited when compared with flare types.

3. Find an alternative manual technique (non-programming) to calculate the total magnetic reconnection flux. Evaluate the results obtained with the prime method, which uses the software package. This effort may give an alternative option to process the data and understand the characteristics of the parameters under study.

1.4 The Scope of Study

The linear correction between magnetic reconnection flux and flare duration (FWHM) against flare classes was examined in 33 flare events that occurred within heliographic longitudes of less than 45°. Equally, a balanced sample size was

examined to align with the purpose, consisting of 17 confined (12 M-classes and 5 X-classes) and 16 eruptives (11 M-classes and 5 X-classes) flares with similar strengths of X-ray peak magnitudes in the long channel 1–8 Å band of GOES X-ray flux. The flare magnitudes correspond to GOES classes M5 to X5, representing both flare types comparably. Their linear correlation relationship is derived, and their coefficient values are compared by flare type. Also, the results have been analyzed in detail using histograms. The event dates occur between February 2011 to September 2017, fall within Solar Cycle 24.

1.5 Thesis Contribution

A balanced sample size between flare types (confined and eruptive) is an important strategy in this study to yield reliable comparison results. The linear correlation coefficient magnitude obtained for the duration and total magnetic reconnection flux reflects their relationship strength against flare class by flare type quantitatively. Flare classes between M5 and X5 have been studied, representing moderate to strong flares, excluding neither weak nor super-flares.

Previous studies concluded that flare duration has no relationship with flare class. In this study, the results have been proven otherwise. Confined flare types show moderate linear correlation (0.58) compared to close-to-no correlation in the eruptive types. Thus, the general assumption that flare duration has no relationship is not conclusive without greater flare magnitude.

Two methods have been explored and compared to calculate the total magnetic reconnection flux, a manual technique (non-programming) and a software package. The manual method is an alternative path to meet the objective. Four events were

examined manually, and the results of those assessments were compared with the computerized results. The software method is the prime tool used to analyze all the 33 events to derive the correlation data in this study. The manual method gives a closer understanding of the HMI characteristic, yet needs further improvements to enhance the result.

1.6 Outline of the Thesis

Chapter 1 briefly outlines the purpose, method, and contribution of this thesis. The scope of the subject is the solar flare duration and total magnetic reconnection flux against flare class.

Chapter 2 explains subjects and explores recent literatures to the thesis. Magnetic reconnection flux and flare duration measurements will be discussed in general.

Chapter 3 details the research approach, method, data collection, flare type selection, data file processing, analysis tools, ethical issues, and research limitations associated with this project. A linear correlation model is used to understand the relationship of the solar flare parameter study.

Chapter 4 analyses the flare duration and total magnetic reconnection flux against flare class linear correlation, and they are compared with variable scope to understand the characteristics based on the results obtained.

Chapter 5 is the simplified summary of the essential points of this study. Thus, this short chapter contains the conclusion of the thesis and future suggestions.

CHAPTER 2

LITERATURE REVIEW

2.1 Introduction

This chapter addresses the key subjects and prior research related to the thesis assessment. It begins with a description of the underlying physics principles, technological support, and literature concerning solar flare monitoring.

2.2 Magnetic Reconnection

When two magnetic fields come into contact, they merge. If two magnets are brought close together, and the strength of the field is measured at some point, you can detect contributions from both. However, magnetic fields have both direction and magnitude; therefore, if two of them have opposite directions, their magnetic field will subtract from each other. When this occurs in a magnetized plasma, the fields can interact in a new way to form new field lines and change their topologies. This process is called magnetic reconnection.

Magnetic reconnection is a fundamental mechanism that occurs naturally in the space sciences, allowing for the huge scale explosive release of energy stored in magnetic fields. The magnetic field rearranges itself during the magnetic reconnection attempt to shift to a lower-energy state. Reconnection enables the release of energy stored in the original stressed magnetic fields. When opposite polarity field lines reconnect and rearrange their magnetic configuration, magnetic energy is immediately transformed into kinetic energy, thermal energy, and acceleration of non-thermal particles (Priest & Forbes, 2002; Shibata & Magara, 2011). The magnetic field's energy is converted to particle motion. This mechanism is found to be important for the sudden release of energy from the solar surface in the form of solar flares and

coronal mass ejections (CMEs). Also, it is believed to be a potential source of heat for the corona, which is exceptionally hot compared to the surface layers below it.

Magnetic fields, like rubber bands, store energy as they are extended. Historically, it was believed that magnetic field lines could never break, regardless of how stretched, they get. In contrast to a rubber band, a single magnetic field line cannot break, as magnetic fields do not have free ends. If another extended magnetic field line in the opposite direction is nearby, they will simultaneously break and cross-connect, maintaining that there is never a free end.

This is illustrated based on Figure 2.1. The top and bottom light blue lines represent magnetic field lines pointing left and right against a backdrop of electric currents. Magnetic field lines pass through the shaded box in the center of Figure 2.1, referred to as the diffusion zone, whereby they effectively break, and the broken ends cross-connect immediately. It is said that the field lines have reconnected. They release their energy by straightening it out to the left and right (Hesse & Cassak, 2020).

The presence of plasma is important for magnetic reconnection. In Figure 2.1, the magnetic field lines thread through the ambient plasma, which is illustrated as light blue circles. When they cross the diffusion zone, the charged particles follow the magnetic field. Since the bent reconnected magnetic field lines stretch out like rubber bands, the plasma mainly moves in the direction of the magnetic field. This results in the formation of two plasma jets that move directly from the diffusion field, as shown by the ovals towards their left and right. As the magnetic field line slings out, it accelerates the plasma at the boundaries of magnetic fields that have already reconnected and those that have not. The jets can reach speeds of up to 1.6 million

km/h, depending on the location of magnetic reconnection in space. Magnetic reconnection also heats the plasma, as shown by the coloring of the plasma in the jets.

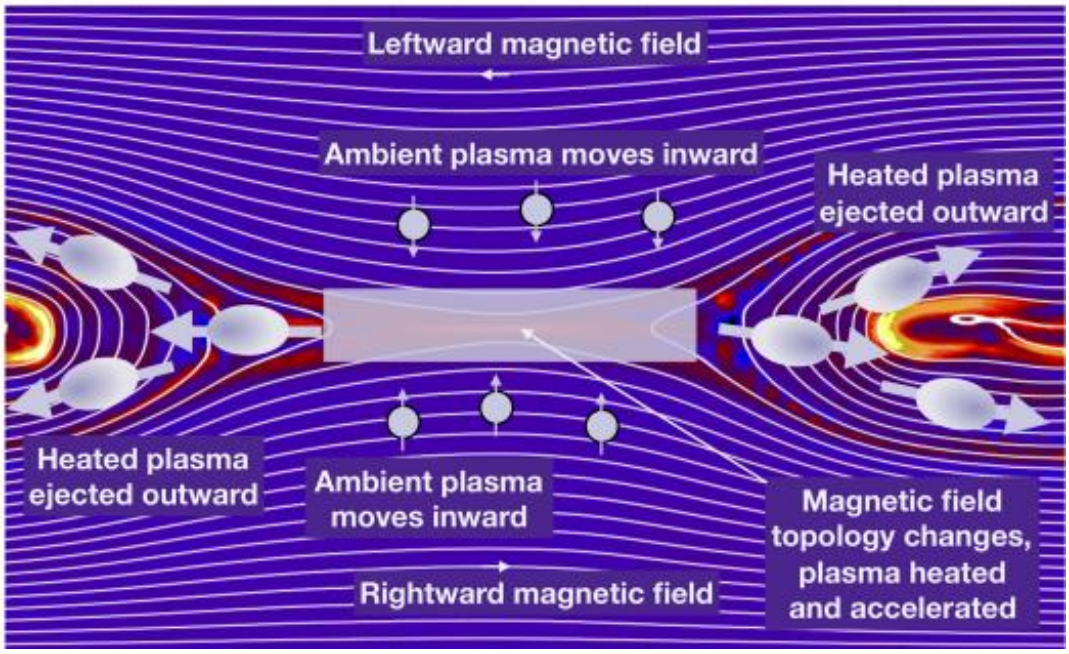

Figure 2.1 Magnetic reconnection in a two-dimensional diagram. Magnetic fields with opposite directions (light lines) and ambient plasma with opposite directions (light circles) travel into the diffusion area (box in the center), where magnetic reconnection occurs. The plasma is heated and accelerated to the left and right in the form of jets (ovals).

Resource: (Hesse & Cassak, 2020)

Heating can occur within the diffusion region or at the interface between connected and unconnected magnetic fields. This heating could be large depending on the environment, up to half of the energy produced by magnetic fields can be used to heat the plasma. Magnetic reconnection is important because it transforms energy efficiently, as well as in the form of directed motion (the jets) and random motion (the increase in temperature). Since it is very common for magnetic fields to change direction, magnetic reconnection happens in a wide range of circumstances. It is the mechanism that generates solar flares, which are massive bursts of light in the Sun's atmosphere that can emit up to 10^{25} J of energy. To put this into perspective, in case

it is possible to harness all of the energy emitted by a single big flare for human use, it could supply enough energy to power the entire planet for about 20,000 years (Hesse & Cassak, 2020).

Magnetic reconnection also occurs in the space surrounding Earth. Earth's magnetic field covers the planet in a bubble, protecting it from the solar wind, a stream of plasma, and magnetic fields originating from the Sun. Magnetic reconnection happens at the bubble's edge when the magnetic field in the solar wind is in the opposite direction of Earth's. This initiates movement of the magnetic field and plasma trapped within Earth's magnetic bubble, accumulating the magnetic field on the side of the Earth pointing away from the Sun. Magnetic fields are again oppositely directed, and magnetic reconnection drives hot plasma toward Earth during geomagnetic storms or substorms. Any of the ambient plasma penetrates down to the Earth's atmosphere, where it excites atmospheric molecules, which then reflect light as they de-excite. This is what explains the aurora lights that are visible near the Earth's poles. As a result, researching magnetic reconnection is essential to understanding the Sun and its impact on the Earth's space environment.

2.3 Solar Flare

The most catastrophic energy-conversion phenomena in the solar atmosphere are solar flares and coronal mass ejections (CMEs). A solar flare is a sudden burst of increased brightness of the Sun, which is typically seen above its surface and near a sunspot group. The magnetic field structure surrounding sunspots is critical for understanding and predicting solar flares. As this structure is twisted and sheared, magnetic field lines will cross and reconnect, resulting in an explosion of energy. The flare (bright area) occurs along a segment of a dividing line between regions of

opposite magnetic fields where the magnetic field is twisted (or sheared). It has been discovered that this shear is a key element in the formation of solar flares (Hathaway, 2014).

Strong flares are sometimes, but not always, followed by coronal mass ejections (CMEs), which their association is still unknown. Solar flares are categorized as eruptive flares when associate with CMEs and confined flares without CMEs. During eruptive flares, the eruption of a magnetic flux rope corresponds to the CMEs, while the heated plasma due to magnetic reconnection is observed as a solar flare. Therefore, the rapid conversion of free magnetic energy stored in the sheared and twisted magnetic fields of active regions leads to solar flare emissions across the whole range of electromagnetic wavelengths (Fletcher et al., 2011; Forbes, 2000; Hudson, 2011; Kazachenko et al., 2012). Solar flare-emitted X-rays and ultraviolet radiation can penetrate the upper Earth's atmosphere (ionosphere), causing bright auroras and even disrupting long-range radio communication.

2.4 Coronal Mass Ejections (CMEs)

The magnetic fields emerge from the Sun, forming enormous arches and loops above its surface. These magnetic loops' build-up and interaction result in an explosion known as coronal mass ejections (CMEs). A CME is the eruption of a massive plasma bubble from the Sun's corona, is one of the most significant impacts of magnetism (Wagner, 1984). They are usually detected with a white-light coronagraph and are correlated with significant changes and disturbances in the coronal magnetic field. Magnetic reconnection is closely associated with CMEs and solar flares, which involve restructuring complex magnetic topologies within the corona (Aarnio et al., 2011).

CMEs and flares are considered different consequences of coronal magnetic field instability and reconnection (Lin et al., 2003; Forbes et al., 2006; Wiegelmann et al., 2014). CMEs may generally occur without flares (Robbrecht et al., 2009; D'Huys et al., 2014), and flares may occur without CMEs (Hudson, 2011; Sun et al., 2015). However, the association rate is a steeply increasing function of the GOES flare class, and both typically occur together in the strongest flare events (Andrews, 2003). A careful statistical study on the CME-flare association was carried out by Yashiro et al. (2006). The results show that the association rate of CMEs with flares is about 50% for M class flares, while the percentage increases up to > 90% for X1.0 class flares and almost 100% for Class X2.0 flares and above.

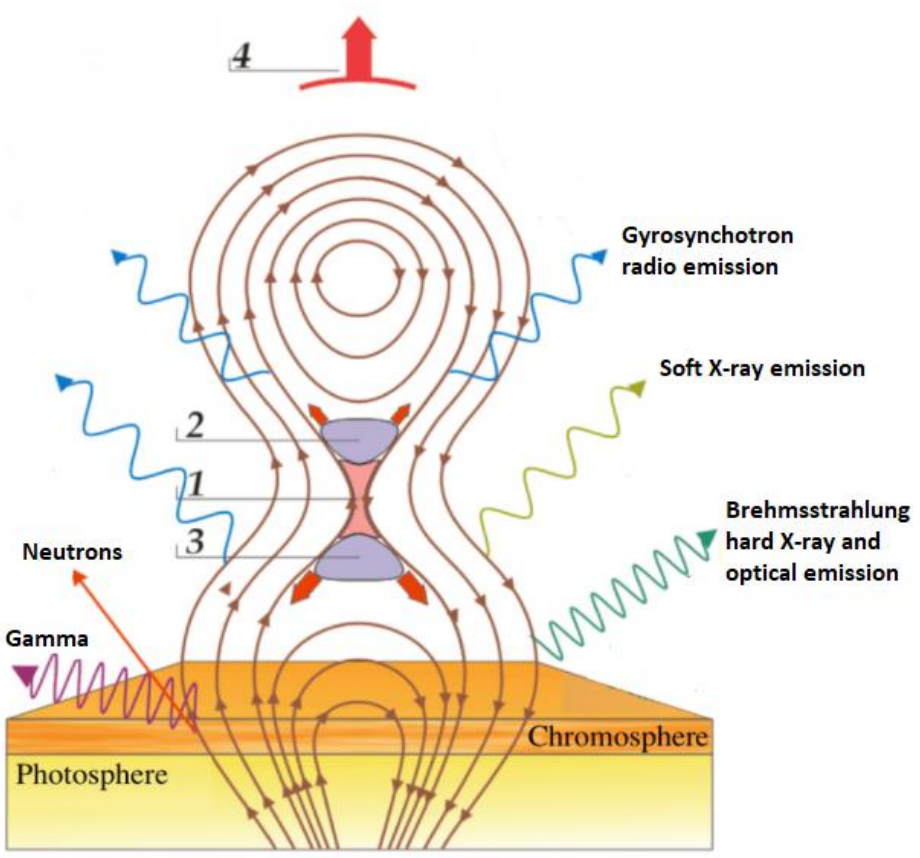

Figure 2.2 Solar flare illustration. 1 - Magnetic reconnection, 2 and 3 - particle acceleration regions above and below the reconnection zone, 4 - CME shock front.

Source: (Bazilevskaya, 2017)

Magnetic reconnection can occur on the Sun's solar arcades, which are a series of tightly packed magnetic lines of force loops. These field lines quickly reconnect into a lower arcade of loops, leaving an unconnected helix of a magnetic field. As shown in Figure 2.2, the sudden release of energy throughout that phase results in the solar flare and ejects a CME. The helical magnetic field and the material within it can violently expand outward, resulting in the formation of a CME. The mass of particles ejected in the CME could amount to 10^{12} Kg, often moving at a speed of hundreds up to several thousand kilometers per second from the Sun (Gosling et al., 1976; Hundhausen et al., 1994; Gopalswamy et al., 2001; Gallagher et al., 2003). This also explains why CMEs and solar flares usually originate in what is known as the Sun's active regions, which have much greater magnetic fields on average.

Before the discovery of modern findings, it was assumed that solar flares caused geomagnetic storms on Earth. As a result, a strong causal relationship between flares and geomagnetic storms was established. However, after the discovery of coronal mass eruptions in the Orbiting Solar Observatory 7 (OSO 7) and Skylab spacecraft observations, it is clear that this relationship is incorrect (Kahler & Hundhausen, 1992; J. Gosling, 1993). Contrary to popular belief, flares are not even needed for coronal mass ejections to occur.

2.5 The Solar Dynamo

Dynamo refers to a system that transforms kinetic energy into electricity. The source of kinetic energy in the Sun is the stirring of turbulent layers of hot ionized gas within the Sun's interior. As a consequence of the movement of ionized gas, these produce electric currents. Ampere's law states that electric currents create magnetic fields. As magnetic fields change, electric currents are induced (Faraday's law). The

dynamo is self-reinforcing in this way, allowing the production of magnetic dipole fields to continue over time. On the Sun's surface and within its interior, some plasma flows were observed. Many of these flows will lead to the formation of the Sun's magnetic field in some way, as long as the loops are not interrupted. However, this is a highly oversimplified version of the theory. There are restrictions on the sorts of velocity fields that can create the performance of the process.

For the dynamo to operate, the plasma flow must have the following properties.

i) Turbulent flows are needed as laminar flows are incapable.

ii) Three-dimensionality is required in the flow.

iii) Helical flows are needed (Seehafer, 1996). By this, it means that the flows must follow a helix's direction. As a result, very complicated flows are needed to produce any magnetic field at all.

iv) Differential rotation is another essential component of dynamo motion. The equator rotates faster than the poles. In other words, the Sun's rotation speed is dependent on its radius and latitude (Schou et al., 1998).

Rubber bands may be used in a variety of ways to convey magnetic field lines. They are made up of tensioned and compressed continuous loop lines of force. Magnetic fields, like rubber bands, can be strengthened by stretching, twisting, and folding into themselves. The Sun's fluid flows show similar stretching, twisting, and folding. Recent solar researchers agreed that the solar dynamo is located in a thin layer of tachocline between the convection and radiative zones. The tachocline's plasma velocity changes will stretch and strengthen the magnetic field line. These conditions are necessary because the plasma's motions must be capable of converting a meridional (poloidal) magnetic field to an azimuthal (toroidal) magnetic field and vice

versa. Supposedly, if it starts with a meridional magnetic field, the Sun's differential rotation twists and coils this field around the Sun, creating an azimuthal magnetic field.

The Omega effect is a pathway that occurs when a meridional magnetic field is converted to an azimuthal one. It is important to the observed solar cycle since the twisting of magnetic flux strands in the azimuthal (toroidal) direction at shallow depths and low latitudes creates intense magnetic "ropes" that are raised to the surface via magnetic buoyancy to generate the bipolar magnetic fields associated with sunspots and other solar cycle-related interaction (Parker, 1955); (Babcock, 1961).

The Alpha effect, on the other hand, converts an azimuthal (toroidal) magnetic field to a meridional (poloidal) field. As of this writing, the exact mechanism of how this happens is still uncertain, but it involves the interaction of the plasma's velocity field, the Sun's rotation, the toroidal magnetic field, and the Coriolis effect acting on rising flux tubes. Both above effects are illustrated in Figure 2.3.

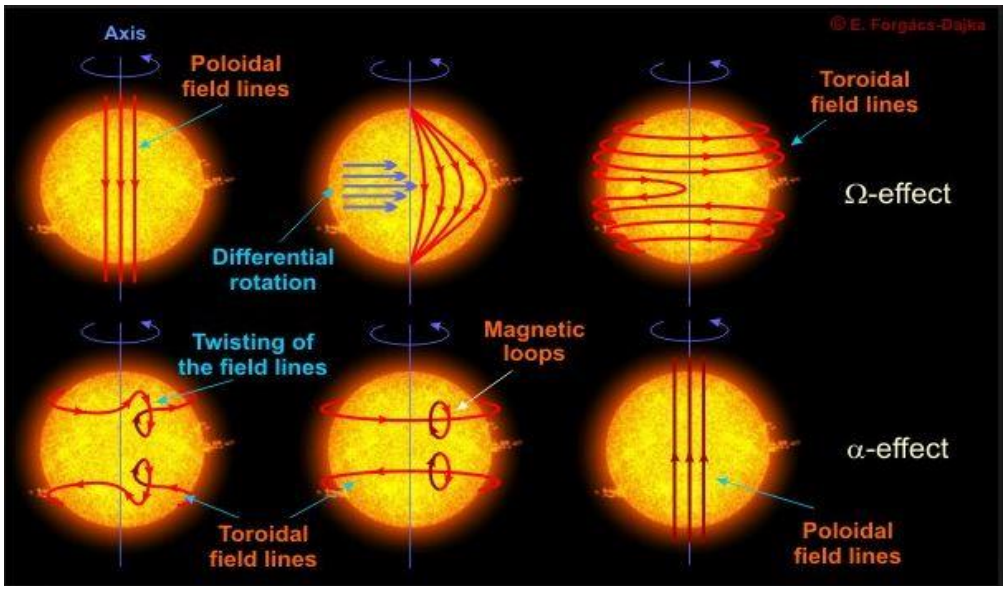

Figure 2.3 The Omega and Alpha effect in the solar dynamo.

Source: (Hulk, 2017).

In a qualitative perspective, assume a sphere of hot plasma rotating at an angular velocity ω. Assume also the fluid is convective and that certain localized pockets are hotter than the surrounding fluid and thus move outward radially at velocity u. Furthermore, consider the existence of a toroidal magnetic field that is dragged partly by the fluid motion. Due to the rotation of the sphere, the Coriolis force $\omega \times u$ exerts an impact on each pocket of fluid, causing it to twist as it moves upwards and expands. Following that, the magnetic field lines twist as well. Since the signs of both the Coriolis force and the toroidal magnetic field are reversed in the northern versus southern hemispheres, both hemispheres have small-scale magnetic field loops of the same polarity. All these small-scale loops of magnetic flux gradually coalesce (combine) due to magnetic diffusivity, leading to the formation of a large-scale poloidal magnetic field (Parker, 1955).

Consequently, a poloidal magnetic field produces a toroidal magnetic field, which regenerates the poloidal magnetic field, and so on. Solar minima are dominated by poloidal fields, while solar maxima are dominated by toroidal fields, which produce sunspots and other solar activity. The cycle repeats approximately every 11 years, and the associated magnetic fields reverse polarity between cycles, resulting in the identified 22-year solar cycle. There are, however, alternative explanations to those described here, and unlike the Omega, the effect was better known. No strong scientific consensus on the exact mechanism of the alpha effect has been yet established.

2.6 The Sun in Different Wavelengths

Sunspots are not the only dynamic features that change in the course of a solar cycle. The chromosphere and corona experience similar dramatic changes. To observe

what occurs in the chromosphere, one must look at the emission lines of elements such as hydrogen and calcium, which emit helpful spectral lines at the temperatures present in that layer. On the other hand, the hot corona can be observed using measurements of X-rays, extreme ultraviolet, and other high-energy wavelengths. In this session, how all the different energy level features on the solar atmosphere are observed and analyzed will be learned.

When a regular camera is used to photograph the Sun, the result is a familiar image: a yellowish, featureless disk, perhaps slightly more red near the horizon due to the light having to pass through more of the Earth's atmosphere and therefore losing blue wavelengths before reaching the camera's lens. Indeed, the Sun emits light in all colors, but since yellow is the Sun's brightest wavelength, that is the color human see through naked eye, or rather, what the camera reflects, because one can never look directly at the Sun. When all visible colors are combined, it is referred to this as "white light." Advanced instruments, either on the ground or in space, can observe light at wavelengths well beyond what the human eye can see. Various wavelengths have been used to paint a complete image of the continuously evolving and changing Sun because it provides information about different components of the Sun's surface and atmosphere.

Yellow-green light with a wavelength of 5500 Å, for example, is usually emitted by a material with a temperature of around 5700 C from the Sun's surface. On the other hand, extreme ultraviolet light at 94 Å originates from atoms at approximately 6 300 000 C and is an excellent wavelength for studying solar flares, which can exceed such high temperatures.

The visible spectrum of light was observed simply because the Sun is formed of heated gas, and similar to an incandescent light bulb, heat produces light. However, when it comes to shorter wavelengths, the Sun emits extreme ultraviolet and X-ray light since it is composed of several types of atoms, each emits light of a certain wavelength once heated to a certain temperature. Not only does the Sun contain a large number of different atoms such as helium, hydrogen, and iron, it also contains various types of ions. When an ion exceeds a certain temperature, it can emit light at unique wavelengths. Since the early 1900s, scientists have cataloged which atoms emit what wavelengths, and the associations are well recorded in lists that can run into hundreds of pages.

Solar telescopes make sense of this wavelength data using two techniques. One of them, known as spectrometers, can analyze several wavelengths of light simultaneously and calculate the amount of each wavelength present. This leads to assessing their temperature ranges represented by the Sun's material. Spectrographs are not like conventional images. Instead, they are graphs that identify the amount of each type of light

On the other hand, devices that produce conventional images of the Sun rely primarily on a single wavelength of light, which is not always apparent to the naked eye. For example, SDO chooses ten distinct wavelengths to observe with its Atmospheric Imaging Assembly (AIA) instrument. Each wavelength is largely determined by a single or possibly two types of ions, while wavelengths emitted by other ions are invariably included. Each wavelength was selected to emphasize a different aspect of the Sun's atmosphere. As shown in Figure 2.4, SDO detects the

following wavelengths (Angstroms), from the Sun's surface outward and their filtergram coverage area is summarised in Table 2.1

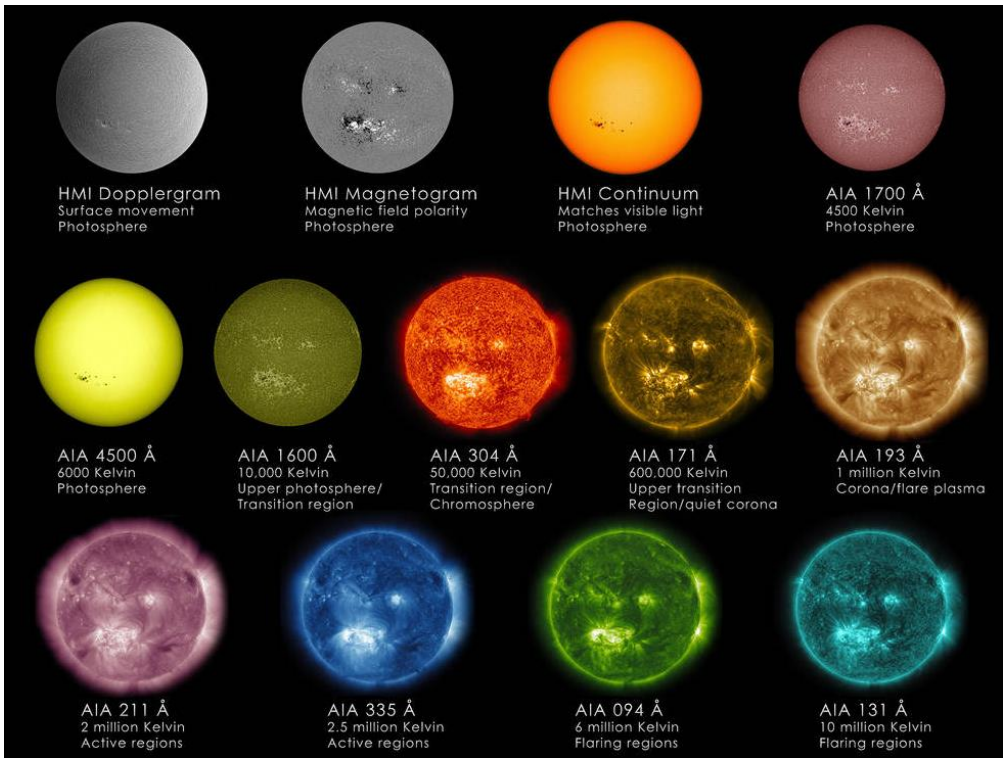

Figure 2.4 SDO shows the Sun in 13 different domains. using two separate onboard equipment.

Source: (Hatfield, 2021)

Table 2.1 SDO filtergram and its sensitive area of coverage.

SDO Filtergram	**Area of correspond**
4500 Å	The Sun's surface, or photosphere
1700 Å	The Sun's photosphere and chromosphere
1600 Å	The chromosphere and the transition zone where temperatures rapidly rise.
304 Å	Between the chromosphere and the transition zone.
171 Å	The Sun's quiet corona and displays coronal loops.
193 Å	The slightly hotter corona and much-heated material related with a solar flare.
211 Å	The Sun's corona's hotter, more magnetically active areas.
335 Å	The corona's hotter, and magnetically active areas.
131 Å	During a flare, this is the hottest material
94 Å	The corona's regions during a solar flare.

Source: (Hatfield, 2021).

2.7 Magnetic Fields Measurement

Up to this point, it has been learned that sunspots have a magnetic property that changes on a cyclic basis. Astronomers have now discovered that solar activity is directly influenced by these dominant mechanisms and their repeated features that continuously drive the Sun's dynamics. It should therefore have a system for calculating the magnetic properties that can be quantified, which will be addressed in the following paragraphs.

An atom has several energy levels and electrons that move from one level to another, creating spectral lines. If each energy level is precisely defined, then the difference between them should also be precisely defined. As a result, a change in the electron level leads to a sharp and narrow spectrum line. These are absorption or emission lines based on whether the energy of the electron increases or decreases during the transition.

The spectral lines discussed so far have assumed that magnetic fields do not influence the atom. However, if a strong magnetic field is present, each energy level can be split into several levels which are very close to one another. The amount of level splitting is proportional to the field's strength. As a product, spectral lines formed in the presence of a magnetic field are a sequence of closely spaced lines corresponding to the subdivisions of the atomic energy levels rather than a single line. The phenomenon of lines splitting in the presence of a magnetic field is called the Zeeman effect (after the Dutch scientist who first discovered it in 1896). Furthermore, the light of each of these divided wavelengths of spectral lines has its desired orientation or circular polarization, which is determined by the direction or polarity of the magnetic field.

Thus, a spectrograph (instrument to obtain astronomical spectrum) can be used to measure the spectral line splitting (Zeeman effect) mentioned above, and a polarizing filter can be used to determine both the magnetic field's strength and direction. This enables one to remotely measure the Sun's magnetic field by measuring the energy difference in the light released when these electrons jump between orbits. Magnetic field lines create a complex network of magnetic structures as they loop through the solar atmosphere and interior. Most of these structures can be seen in the corona and chromosphere. Typically, however, the magnetic field is directly measured in the photosphere (Figure 2.5) (Scherrer, 2008).

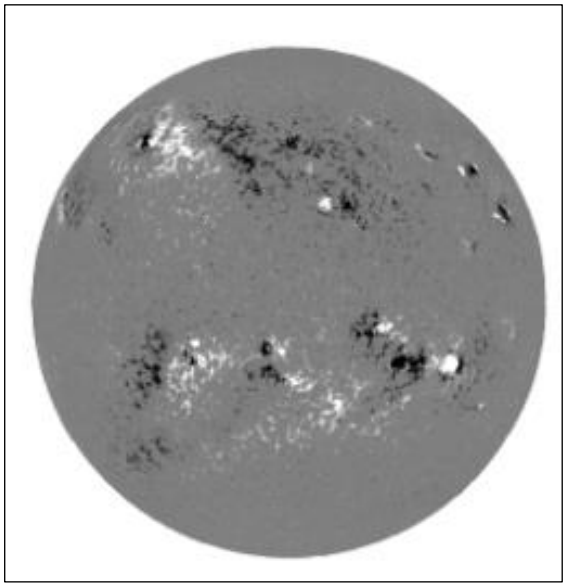

Figure 2.5 Magnetogram Image. The magnetic field on the Sun's surface, with black lines pointing away from Earth and white lines pointing toward Earth.

Source: (Scherrer, 2008)

Therefore, the magnetic fields across the Sun's surface can be measured with the appropriate instrumentation. Magnetograms are images of the photosphere's magnetic field. It's a photograph taken by a device that can reflect the polarity and strength of the magnetic fields on the Sun. One such instrument that generates

magnetograms from its observations is the Helioseismic and Magnetic Imager (HMI) instrument aboard the Solar Dynamics Observatory (SDO) satellite. Daily magnetograms from this instrument are available through their website, one of the primary sources of material used in this thesis.

2.8 Solar Flare Classification

Flares generate electromagnetic radiation with wavelengths ranging from radio waves to gamma rays. The majority of the energy is distributed outside the visual range, and therefore commonly, flares are invisible to the naked eye unless using a specialized instrument to detect.

The NOAA space environment center monitors solar flares through their Geostationary Operational Environmental Satellites (GOES, Donnell et al., 1977). GOES satellite is equipped with two X-ray Sensors (XRS) to measure X-ray wavelength in the ranges 0.5 to 4 Å (short channel) and 1 to 8 Å (long channel). The GOES XRS onboard detect solar flare's intensity and classify as A, B, C, M, or X according to their peak flux (Wm^{-2}) of 1 to 8 Å X-rays near Earth (Figure 2.6). Measurements in these bands have been made by NOAA satellites since 1974 (Aschwanden, 1994). Therefore, their long channel archive data have been used in this study.

Each X-ray class is classified on a logarithmic scale ranging from 1 to 9. For instance, B1 to B9, C1 to C9, and so forth. An X3 flare is tripple the magnitude of an X1 flare and six times the power of an M5 flare. The X-class classification scheme is slightly different, it does not stop at X9 but continue moves on. Solar flares of an X10 or greater magnitude are sometimes referred to as Super X-class solar flares.

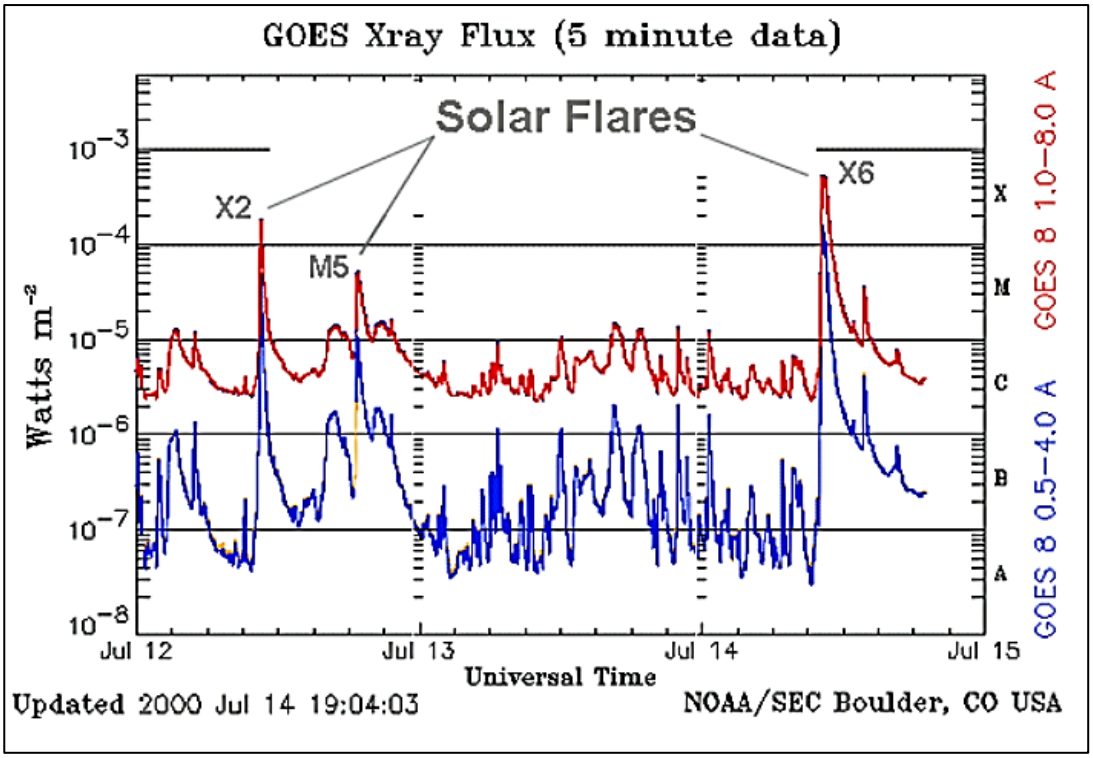

Figure 2.6 GOES X-ray flux shows a series of flare classes of channel 1 to 8 Å detected by NOAA satellite in July 2000.

Source: (Dana, 2000).

Solar flare classification referring to their X-ray flux at peak magnitude as shown in the Table 2.2. The two lowest classes of solar flares are A and B. The smallest ones are A-class which is very common and not very popular as it is near to the background flux (the amount of radiation emitted when there are no flares). Similar to this B-class is usually in the range of background flux level during solar maximum. The C-class solar flares are minor solar flares that rarely affect Earth except for those with a long flare duration that may trigger a weak coronal mass ejection. M-class flares are moderate category flare, it generally causes brief radio blackouts and once in a while a minor radiation storm. The X-class flares are strong with significant events and long-lasting radiation flares in the upper atmosphere (https://www.spaceweatherlive.com/en/help/what-are-solar-flares.html).

Table 2.2 Solar Flare Classification by GOES 1 to 8 Å X-ray's channel.

Flare Class	Peak flux range (Wm^{-2}) between 1 - 8 Angstroms
A	$< 10^{-7}$
B	10^{-7} to 10^{-6}
C	10^{-6} to 10^{-5}
M	10^{-5} to 10^{-4}
X	$> 10^{-4}$

Source: https://www.spaceweatherlive.com/en/help/what-are-solar-flares.html

2.9 Magnetic Reconnection's Flare Ribbon Evolution

In solar flare/CME events, the evolution of flare ribbons followed by their separation is one of the most common observation signatures of the magnetic reconnection process (Fletcher et al., 2011; Hinterreiter et al., 2018). The flare ribbon evolution provides indirect evidence of the magnetic reconnection process, which could be detected by Hα, Extreme Ultraviolet (EUV), and hard X-ray (HXR) wavelengths (Benz, 2016; Holman, 2016). According to Toriumi et al. (2017), when the area of flare ribbons normalized by the sunspot area is large, solar flares tend to be accompanied by CMEs.

The flare ribbons mark the chromosphere foot-points of the newly reconnected magnetic field at the coronal region. They are caused by energetic particles transported downward along the field lines, particularly by accelerated electron beams (Priest & Forbes, 2002; Shibata & Magara, 2011). The CSHKP model, based on works by Carmichael (1964), Sturrock (1966), Hirayama (1974), and Kopp & Pneuman (1976), is the most widely accepted model for the physical processes in eruptive two-ribbon flares.

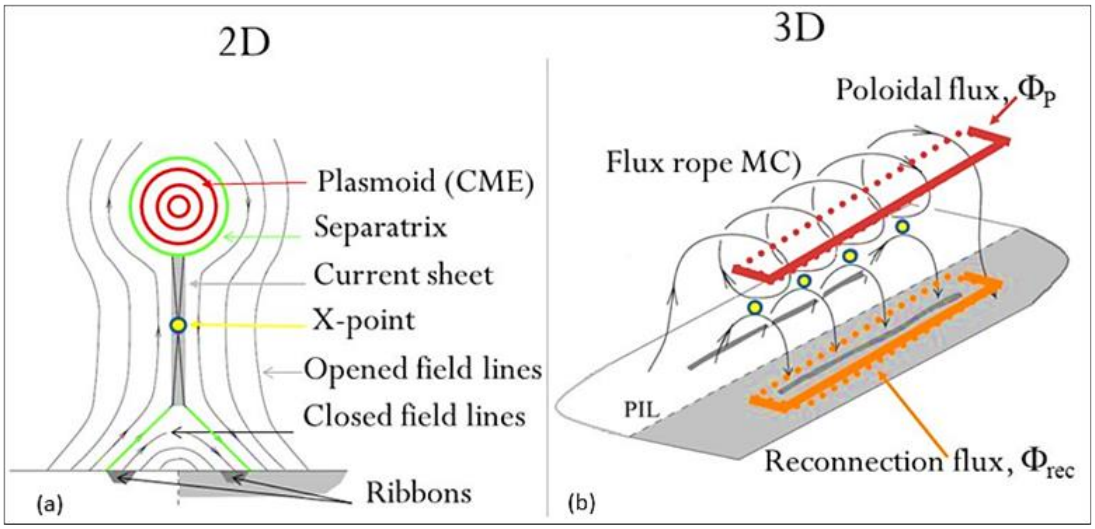

Figure 2.7 The CSHKP two-ribbon flare fundamental models in 2.7(a) two-dimension and 2.7(b) three-dimension. Ribbons indicate the location of the flare. Closed field lines are the coronal flare loops formed by magnetic reconnection. Opened field lines are the overlying arcade, PIL is the polarity inversion line, X-point magnetic reconnection site(s), and closed field lines are the coronal flare loops formed by magnetic reconnection.

Resource: 2.7(a) (Forbes, 2000) and 2.7(b) (Longcope et al., 2007)

Figure 2.7(a) explains both standard and large-scale observational parameters of solar flares. In addition, many three-dimension (3D) generalizations of the CSHKP scenario have been described in the context of cartoons (Moore et al., 2001), analytical flux rope approaches (Isenberg & Forbes, 2007), and quantitative topological models (Longcope et al., 2007). Figure 2.7(b) illustrates the schematic of the CSHKP to show the reconnection occurs at several locations to develop 3D flare arcade loops and erupting CME flux rope (Longcope et al., 2007).

Figure 2.7 shows one of the main characteristics of a solar flare: the amount of magnetic flux involved in reconnection. The reconnected flux cannot be directly measured from the corona observations. Therefore the CSHKP model function as a quantitative method to correlate the reconnection flux in the corona and the magnetic